Crater FTEs:

Simulation Results and THEMIS Observations

D. G. Sibeck[1], M. Kuznetsova[1]

V. Angelopoulos[2], K.-H. Glaßmeier[3], and J. P. McFadden[4]

[1]Code 674, NASA/GSFC, Greenbelt, MD

[2]IGPP, UCLA, Los Angeles, CA

[3]Technical University, Braunschweig, Germany

[4]SSL, UCB, Berkeley, CA

Abstract

The BATS-R-US magnetohydrodynamic (MHD) model predicts flux transfer events (FTEs) with strong core magnetic fields embedded within a broadened current layer with weak magnetic field strengths on the equatorial dayside magnetopause during intervals of southward and duskward interplanetary magnetic field (IMF) orientation. Multipoint THEMIS observations at 2202 UT on June 20, 2007 of a southward-moving FTE on the post-noon magnetopause confirm the predictions of the model. Magnetosheath spacecraft THEMIS-E and –A with large impact parameters simply observe magnetic field strength enhancements, magnetospheric spacecraft –B and –C with moderate impact parameters observe crater FTEs with deep troughs bounding a strong core field, while THEMIS-D with a very low impact parameter observes only the core magnetic field strength enhancement.

1. Introduction

Component reconnection models predict reconnection along extended lines passing through the vicinity of the subsolar point on the dayside magnetopause. The lines tilt in response to the IMF orientation, running from southern dawn to northern dusk during periods of duskward IMF orientation [Sonnerup, 1974]. Reconnection along extended parallel x-lines generates flux ropes of spiraling magnetic fields [Lee and Fu, 1985]. When there is no guide field, magnetic field strengths within the core region are weak [Ding et al., 1991]. When there is a guide field, the newly reconnected magnetic field lines sweep up magnetosheath field lines in their path to create core regions with large magnetic field strengths [Scholer, 1988].

The newly reconnected magnetic field lines within bubbles and flux ropes move under the influence of pressure gradient and magnetic curvature forces. Spacecraft that remain outside passing events should observe transient enhancements in the draped magnetic field strength and bipolar magnetic field perturbations in the direction normal to the nominal magnetopause [Farrugia et al., 1987]. Spacecraft that enter the events should observe the characteristic bipolar magnetic field signature, a mixture of magnetosheath and magnetospheric plasmas, and either an enhancement (in the case of swept-up magnetic fields) or a crater-like variation (in the case of antiparallel magnetosheath and magnetospheric magnetic fields) in the total magnetic field strength. Plasma flows within the events should be in the direction of event motion, whereas flow perturbations in the ambient media on the flanks of the events should be in the direction opposite event motion [Sibeck and Smith, 1992].

Observations in the vicinity of the dayside magnetopause during periods of southward IMF orientation confirm that FTEs with enhanced or crater-like magnetic field strength variations are common [Russell and Elphic, 1978; Rijnbeek et al., 1987]. However, some FTEs exhibit more complicated crater-like structures in which magnetic field strength enhancements bound trenches which in turn bound slight increases in the field at the center [Labelle et al., 1987].

This paper addresses the latter type of event. It presents results from a high spatial resolution global MHD simulation that predicts the formation of an isolated FTE between tilted reconnection lines passing through the subsolar magnetopause. The magnetic field strength within the core of this event is not slight, but rather far greater than that in the neighboring magnetosphere. This core region magnetic field lies embedded within the weak magnetic field strength of the current layer. The event bulges outward, causing magnetic field strength enhancements in the surrounding regions. Consequently, spacecraft in the outermost magnetosphere that enter the event should observe magnetic field strength enhancements bounding trench-like magnetic field strength decreases, which in turn bound a strong core magnetic field. Multipoint THEMIS observations in the vicinity of the dayside magnetopause on May 20, 2007 confirm these predictions of the model, and provide evidence for the reverse flow perturbations expected on the flanks of the event.

2. MHD simulation

We describe predictions of the Block-Adaptive-Tree-Solarwind-Roe-Upwind-Scheme (BATS-R-US) MHD model developed at the Center for Space Environment

Modeling of the University of Michigan [Powell et al., 1999]. BATS-R-US employs an adaptive grid composed of rectangular blocks arranged in varying degrees of spatial refinement. We set the grid resolution to 1/16 R_E in the vicinity of the dayside and flank magnetopause. The model derives ionospheric electric potentials and conductances from magnetospheric field-aligned currents. We set the Pedersen and Hall conductivities to constant 5 and 0 mhos, respectively. There is no dipole tilt. The solar wind density, velocity, and temperature remain constant at 2 cm^{-3}, 300 km s^{-1}, and $2x10^5$ K, respectively.

Figure 1 shows the predictions of the model for a cut through the noon meridional plane at a time 80 min after the IMF turned from due northward to southward and duskward (Bx, By, Bz = 0, 4.33, -2.5) nT. The magnetopause, a layer of depressed (10-15 nT) magnetic field strengths running from (x, z) = (6, 12.5) to (14, 2) and (-4, 13) to (-1, 14) R_E separates the magnetospheric region of strong northward magnetic fields on the left from the magnetosheath regions of weak southward magnetic fields to the right. A flux rope whose core region contains magnetic field strengths (~40 nT) greater than those in either the nearby magnetosphere or magnetosheath, lies centered on the subsolar magnetopause at (14, 0.6) R_E with dimensions of about ~2 R_E normal to the magnetopause and ~1 R_E along it. Magnetic field lines spiral around this flux rope, which protrudes much further into the magnetosheath than the magnetosphere. Magnetosheath magnetic field strengths are enhanced within a broad region of field lines draped over the flux rope. Note that the axis of the flux rope does not lie perpendicular to the meridional cut shown in the figure. Instead, it runs from southern dawn to northen dusk, parallel to the reconnection line predicted for the component reconnection model for the given IMF orientation.

Magnetosheath plasma flows north north of the event and south south of the event (not shown). By contrast, plasma within the current layer flows equatorward into the flux rope. Flux rope densities are comparable to those in the outer magnetosphere, and far less than those in the magnetosheath.

Figure 2 presents the time history of magnetic field strength variations expected at three points within the simulation box. Spacecraft with large impact parameters that remain outside the event, e.g. (X, Z) = (2, 16), should observe a slight increase in the total magnetic field strength. Spaceraft with moderate impact parameters that enter the event, e.g. (X, Z) = (2, 14), should observe a strong core magnetic field strength flanked by deep troughs. Spacecraft with very low impact parameters that begin and end the interval in the current layer, e.g. (X, Z) = (2, 13.5), should observe a large enhancement in the total magnetic field strength. All three spacecraft should observe bipolar magnetic field signatures in the direction normal to the nominal magnetopause, but these signatures are strongest for the spacecraft with low impact parameters.

3. Observations

At 2202 UT on May 20, 2007, the five THEMIS spacecraft were arrayed nearly perpendicular to the nominal magnetopause as they moved inbound at post-noon local times along their common equatorial coast-phase orbit. Table 1 lists their positions. In order of increasing distance from Earth, the spacecraft were arrayed as follows: THEMIS-B, THEMIS-C, THEMIS-D, THEMIS-E, and THEMIS-A. The difference in radial distances from Earth of THEMIS-B and -A was 0.65 R_E.

Table 1

Spacecraft	GSM X	GSM Y	GSM Z	R (R_E)
THEMIS-A	6.23	12.88	1.62	14.40
THEMIS-B	4.99	12.70	1.70	13.75
THEMIS-C	5.06	12.79	1.70	13.86
THEMIS-D	5.42	12.80	1.68	14.00
THEMIS-E	6.02	12.95	1.63	14.37

Figure 3 presents THEMIS-A to –E magnetic field observations [Auster et al., 2008] in boundary normal coordinates, where **l** lies in the plane of the magnetopause and points in the direction of the magnetospheric magnetic field, **n** lies normal to the magnetopause and points outward, and **m** completes the triad by pointing dawnward [Russell and Elphic, 1978]. THEMIS-B and C (solid and dashed blue traces, respectively) observed a strong steady northward magnetospheric magnetic field prior to 2202 UT and after 2202:30 UT with (Bl, Bm) = (30, 0) nT, whereas THEMIS-E and A (dashed and solid black traces, respectively) observed a southward and duskward magnetosheath magnetic field during the same intervals with (Bl, Bm) = (-20, -10) nT. The large (~150°) shear angle between these ambient magnetospheric and magnetosheath magnetic fields favored magnetic reconnection. Prior to 2202 UT and between 2202:30 and 2204 UT, THEMIS-D (red trace) lay within the magnetopause current layer, where the north/south component of the magnetic field oscillated between values weaker than those in either the magnetosheath or the magnetosphere. After 2204 UT, THEMIS-D joined THEMIS-B and –C in the magnetosphere.

From 2202 to 2202:30 UT, all five THEMIS spacecraft observed an FTE marked by bipolar (-,+) Bn signatures normal to the nominal magnetopause. These signatures were most pronounced at THEMIS-D within the current layer, but were also large at THEMIS-B and –C. At THEMIS-E and –A, the initial negative pulse was weak and protracted, but the subsequent positive pulse was comparable to that seen by the other spacecraft.

THEMIS-B and –C observed crater-like magnetic field strength variations similar to those discussed by Labelle et al [1987], in which field strength increases bounded trenches, which in turn bounded a central peak. The duration of these signatures was longer, and the central peak higher, at THEMIS-C than THEMIS-B, suggesting that THEMIS-C passed closer to the center of the event than THEMIS-B. Note that THEMIS-B and –C observed positive (dawnward) Bm deflections within the core region of the event.

By contrast, THEMIS-E and –A remained in the magnetosheath throughout the event. Here they observed nothing more than an enhanced negative (or duskward) Bm component. THEMIS-D, previously in the current layer, observed magnetic field strengths greater than those in either the magnetosheath or the magnetosphere. Within the core region of the event, the magnetic field pointed in the (Bl, Bm) = (40, -45) nT direction. The field strength within the core region of this event is consistent with the MHD model predictions reported above, but much stronger than those seen in the events reported by Labelle et al. [1987].

Figure 4 presents the plasma velocities observed by electrostatic analyzer [McFadden et al., 2008] on THEMIS for the same 5-minute time interval. THEMIS-E and –A remained within the magnetosheath throughout the interval, where they observed southward and duskward flows, (Vl, Vm) = (-150, -100 to -200) km/s. THEMIS-B and –C observed weak flows within the magnetosheath, but flows very similar to those in the magnetosheath while within the FTE from 2202 to 2202:30 UT. Black arrows in the top panel indicate times just prior to and after the event when THEMIS-B and –C observed northward flows. In the current sheet, THEMIS-D observed very weak flows prior to the arrival of the FTE, flows similar to those in magnetosheath while within the FTE, and strong southward flows after the FTE from 2202:30 to entry into the magnetosphere at 2204:20 UT. With the possible exception of a brief outward flow seen by THEMIS-B at 2202 UT, none of the spacecraft observed any significant flows normal to the nominal magnetopause.

4. Discussion

THEMIS-E and A observed a southward and duskward magnetosheath magnetic field. According to the component reconnection model, this should have resulted in reconnection along tilted subsolar reconnection lines running from southern dawn to northern dusk. If reconnection along two or more lines resulted in the formation of an FTE then the axis of the FTE should also have run from southern dawn to northern dusk. At equatorial post-noon locations, the THEMIS spacecraft were located south of the nominal reconnection line(s) and should only have been able to observe southward moving events.

THEMIS observations confirm the predictions of the component reconnection model: the magnetic field orientation observed by THEMIS-D within the core region of the event pointed northward and duskward, indicating an FTE whose axis ran from southern dawn to northern dusk. The reverse (inward/outward) bipolar signatures seen by all the spacecraft indicate southward event motion [e.g., Rijnbeek et al., 1982].

Plasma observations also confirm the southward motion of the event. Upon entering the event, THEMIS-B and –C observed southward and duskward flows similar to those seen by THEMIS-E and A in the nearby magnetosheath, indicating that the event is moving with the background magnetosheath flow rather than in a direction determined by magnetic curvature forces. However, both THEMIS-B and –C observed strongly northward flows in the magnetosphere just before entering the event and slightly northward flows upon reentering the magnetosphere. We interpret these northward flows as evidence for the flows opposite event motion in the ambient media that are expected on the flanks of FTEs.

The magnetic field within the event was twisted about the axial field. Whereas THEMIS-B and –C observed dawnward magnetic field perturbations within the trenches on the Earthward side of the event, THEMIS-E and –A observed duskward magnetic field perturbations on the magnetosheath side of the event. While the northward and duskward pointing core magnetic field within the events can result from a smooth rotation from the southward and duskward magnetosheath to the northward magnetospheric magnetic field orientations within the event, it is difficult to see how it can result from interconnected magnetosheath-magnetospheric magnetic field lines 'snow-plowing' unreconnected southward and duskward magnetosheath magnetic field lines in their path.

However, even a rotation between the magnetosheath and magnetospheric magnetic field orientations cannot explain the dawnward tilting magnetic field lines within the trenches on the Earthward side of the event. Although Saunders et al. [1984] invoked Alfvén waves to explain correlated field and flow signatures within FTEs, this event provides no evidence for the required plasma fluctuations. It seems more likely that the tilts in the magnetic field orientations seen within the trenches and magnetosheath simply result from draping over the core region. Since only the component of the magnetic field transverse to the event axis increases, draped magnetic fields rotate towards directions perpendicular to that axis. In the present case, the northward magnetospheric magnetic field backs dawnward in the presence of an event with an axis running from southern dawn to northern dusk, while the strongly southward magnetosheath magnetic field veers duskward.

Finally, we note that Lui et al. [2008] employed a reconstruction technique based on the Grad-Shafronov equation and THEMIS-D plasma and magnetic field observations to demonstrate that the core region of this same FTE has spatial dimensions ~2000 km along and perpendicular to the magnetopause, a core magnetic field strength exceeding 50 nT, and an axial current density > 40 nA/m^2.

5. Conclusion

We presented THEMIS observations of an FTE on the afternoon magnetopause whose internal structure, including a strong core magnetic field bounded by weak troughs, agrees well with MHD model predictions. For the observed duskward and southward magnetosheath magnetic field orientation, the component reconnection model predicts southward-moving events at the equatorial post-noon location of the THEMIS spacecraft. Both bipolar (inward/outward) magnetic field signatures normal to the nominal magnetopause and in situ flow perturbations indicate that the event was indeed moving southward and duskward on the magnetopause. Although the event itself is moving with the background magnetosheath flow, the high speeds flows seen within the magnetopause current layer indicate that reconnection continued after the event's passage. Northward flows just inside the magnetosphere on the edges of the event are consistent with the reverse flows expected on the flanks of southward-moving events.

Acknowledgments. It is a pleasure to acknowledge the enthusiastic support of the THEMIS project and science teams throughout the course of the mission.

References

Auster, U., et al., The THEMIS fluxgate magnetometer, Space Sci. Rev., submitted, 2008.

Ding, D.-Q., L.-C. Lee, and Z.-W. Ma, Different FTE signatures generated by the bursty single-x line reconnection and the multiple-x line reconnection at the dayside magnetopause, J. Geophys. Res., 96, 57-66, 1991.

Farrugia, C. J., R. C. Elphic, D. J. Southwood, and S. W. H. Cowley, Field and flow perturbations outside the reconnected field line region in flux transfer events: Theory, Planet. Space Sci., 35, 227-240, 1987.

Labelle, J., R. A. Treumann, G. Haerendel, et al., AMPTE IRM observations of waves associated with flux transfer events in the magnetosphere, J. Geophys. Res., 92, 5827-5843, 1987.

Lee, L.-C. and Z.-F. Fu, A theory of magnetic flux transfer at the Earth's magnetopause, Geophys. Res. Lett., 12, 105-108, 1985.

Lui, A. T. Y., et al., Reconstruction of a magnetic flux rope from THEMIS observations, Geophys. Res. Lett., submitted, 2008.

McFadden, J. P., et al., THEMIS ESA first scienc resultts and performance issues, Space Sci. Rev., submitted, 2008.

Powell, K. G., P. L. Roe, T. J. Linde, T. I. Gombosi, and D. L. De Zeeuw, A solution adaptive upwind scheme for ideal magnetohydrodynamics, J. Comp. Phys., 154, 284-309, 1999.

Rijnbeek, R. P., S. W. H. Cowley, D. J. Southwood, and C. T. Russell, Observations of reverse polarity flux transfer events on the dayside magnetopause, Nature, 300, 23-26, 1982.

Rijnbeek, R. P., C. J. Farrugia, D. J. Southwood, M. W. Dunlop, W. A. C. Mier-Jedrzejewicz, C. P. Chaloner, D. S. Hall, and M. F. Smith, A magnetic boundary signature within flux transfer events, Planet. Space Sci., 35, 871-878, 1987.

Roelof, E. C. and D. G. Sibeck, Magnetopause shape as a bivariate function of interplanetary magnetic field Bz and solar wind dynamic pressure, J. Geophys. Res., 98, 21421-21450, 1993.

Russell, C. T. and Elphic, R. C., Initial ISEE magnetometer results: Magnetopause observations, Space Sci. Rev., 22, 681–715, 1978.

Saunders, M. A., C. T. Russell, and N. Sckopke, Flux transfer events- Scale size and interior structure, Geophys. Res. Lett., 11, 131-134, 1984.

Scholer, M., Strong core magnetic fields in magnetopause flux transfer events, Geophys. Res. Lett., 15, 748-751, 1988.

Sibeck, D. G., and Smith, M. F., Magnetospheric plasma flows associated with boundary waves and flux transfer events, Geophys. Res. Lett., 19, 1903-1906, 1992.

Sonnerup, B. U. O., Magnetopause reconnection rate, J. Geophys. Res., 79, 1546-1549, 1974.

Figure captions.

Figure 1. MHD simulation predictions for magnetic field strengths and vectors and vectors in the noon-midnight meridional plane in the vicinity of an FTE.

Figure 2. Variations in the magnetic field strength and x-component of the magnetic field along the cuts through Figure 1. For times after the encounter with the event, the sense of the x-component has been reversed.

Figure 3. THEMIS-B (solid blue), -C (dashed blue), -D (red), -E (dashed black), and –A (solid black) observations of the magnetic field in boundary normal components from 2200 to 2205 UT on May 20, 2007.

Figure 4. THEMIS-B (solid blue), -C (dashed blue), -D (red), -E (dashed black), and –A (solid black) observations of the ion velocity in boundary normal components from 2200 to 2205 UT on May 20, 2007.

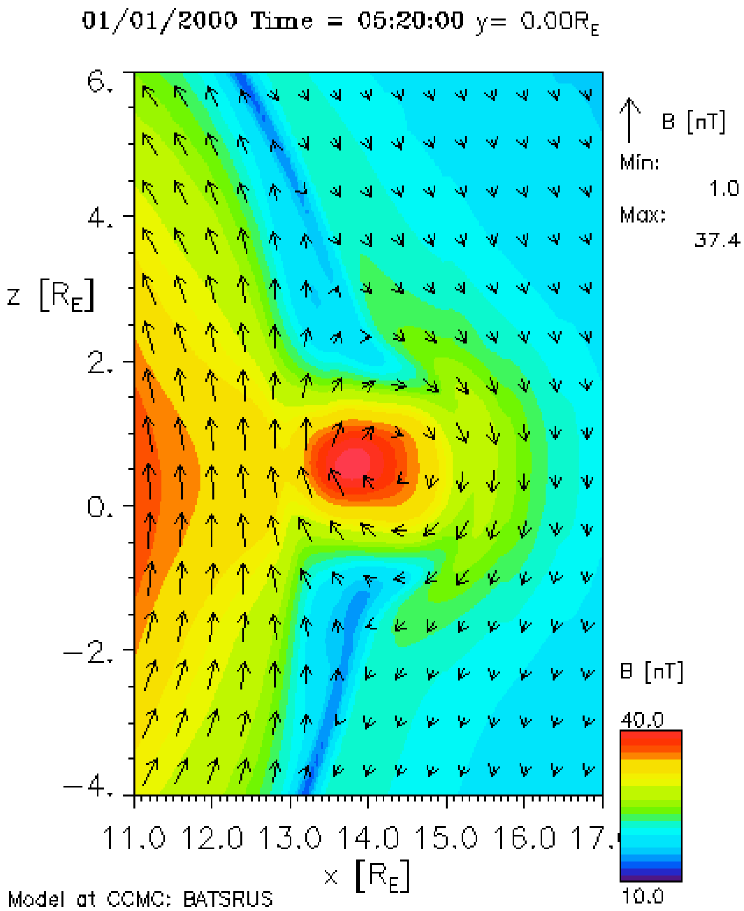

01/01/2000 Time = 05:20:00 y= 0.00R$_E$
z [R$_E$]
6.
4.
2.
0.
−2.
−4.
11.0 12.0 13.0 14.0 15.0 16.0 17.
x [R$_E$]
B [nT]
Min:
1.0
Max:
37.4
B [nT]
40.0
10.0
Model at CCMC: BATSRUS

figure 1.

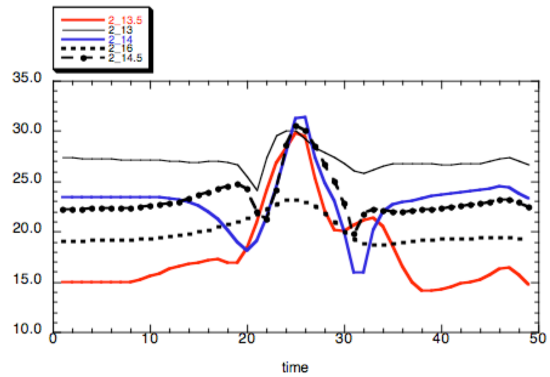
2_13.5
2_13
2_14
2_16
2_14.5
35.0
30.0
25.0
20.0
15.0
10.0
0
10
20
30
40
50
time

Figure 2

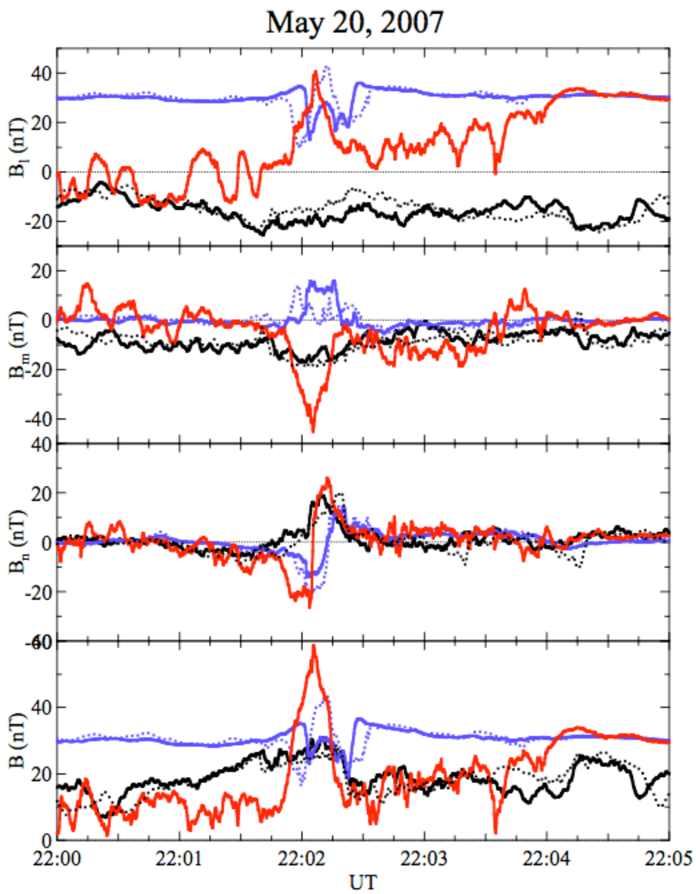
May 20, 2007
B_l (nT)
B_m (nT)
B_n (nT)
B (nT)
40
20
0
-20
-40
60
22:00
22:01
22:02
22:03
22:04
22:05
UT

Figure 3

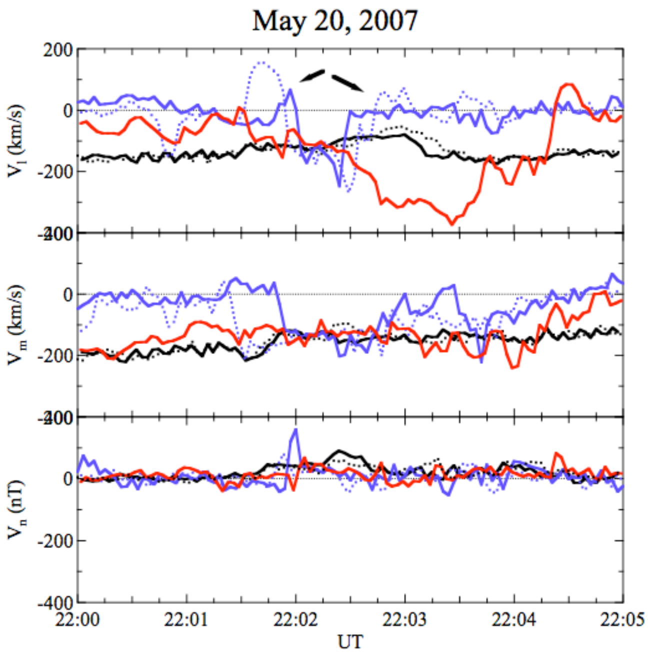
May 20, 2007
200
0
-200
-400
V_l (km/s)
V_m (km/s)
V_n (nT)
22:00
22:01
22:02
22:03
22:04
22:05
UT

Figure 4.